Advance Sustainable Science, Engineering and Technology (ASSET)
Vol. 7, No.3, July 2025, pp. 0250306-01 ~ 0250306-09
ISSN: 2715-4211 DOI: https://doi.org/10.26877/asset.v7i3.1809

Analysis Stability of Retaining Wall type Soldier Pile during Dewatering Work on Hospital Construction Site

Yulia Putri Ramadhani[1*], Dian Purnamawati Solin[1], Yerry Kahaditu Firmansyah[1], Hoang-Khanh Le[2, 3]

[1]Department of Civil Engineering, Faculty of Engineering, Universitas Pembangunan Nasional "Veteran" Jawa Timur, Surabaya 60294, Indonesia

[2]Department of Civil Engineering, National Yang Ming Chiao Tung University, Hsinchu, Taiwan

[3]Faculty of Civil Engineering, Can Tho University, Can Tho, Vietnam

*diansolin.ts@upnjatim.ac.id

Abstract. Groundwater subsidence during dewatering work can be a serious challenge if soil conditions are unstable, potentially disrupting the stability of supporting structures such as soil retaining walls. This research analyzed the stability of soldier pile type soil retaining walls during the dewatering process in hospital construction projects in the BSD area. The data used included the results of Standard Penetration Test (N-SPT), monitoring of dewatering work, inclinometer readings, and stability analysis using a 2D-based finite element software. The simulation results showed that the decrease in the groundwater level caused a change in lateral pressure on the retaining wall, with the maximum deformation reaching 2 m and the safety factor dropping from SF = 2.5 to SF = 2.2. If the analysis indicates a critical impact on stability (SF < 1.5 or deformation exceeding tolerances), then mitigation measures such as the installation of additional struts or dewatering system optimization are required. These findings provide technical guidance to minimize the risk of structural failure during the dewatering process on softsoils.

Keywords: slope stability, dewatering, finite element software, geotechnical stability, soil mechanics, groundwater management system

(Received 2025-03-22, Revised 2025-04-30, Accepted 2025-04-30, Available Online by 2025-05-22)

1. Introduction

The dewatering process in underground construction has become a major concern in geotechnical engineering due to its impact on the stability of the surrounding soil [1]. Recent studies have shown that a decrease in groundwater levels during dewatering can lead to significant changes in the effective stress distribution of soils, which directly affects the performance of soil retaining structures [2]. This

phenomenon becomes increasingly complex when it occurs in layered soils with heterogeneous hydrogeological characteristics, such as those often encountered in large-scale construction projects [3]. In the case of the construction of a hospital in BSD, field observations showed significant landslides around the dewatering site, but the exact mechanism linking the dewatering process to this phenomenon is still not fully understood [4].

A critical review of the relevant literature reveals some limitations in previous research. The development of a model to predict soil deformation due to dewatering, but the model is only valid for coarse-grained soils and has not been tested on clay soil conditions such as at the research site [5]. Previous studies of soldier pile-type soil retaining walls have provided valuable insights, but have not considered the combined effects between long-term dewatering and the creep properties of clay soils [6]. Further, previous studies have tended to use a simple analytical approach that ignores the complex interactions between soil retaining structures, soils, and dewatering systems [7]. This knowledge gap is the rational basis of current research.

The main problem faced in this project is the uncertainty in predicting the behavior of the soil retaining wall during the dewatering process, especially in terms of: (1) the magnitude and distribution of soil deformation [8]; (2) changes in lateral pressure on the retaining wall; and (3) the long-term impact on the stability of the structure. This study aims to develop a numerical analysis model based on the finite element method (FEM) software that is able to comprehensively simulate the behavior of the soil-retaining wall-dewatering system, by including critical parameters such as variations in layered soil permeability, clay soil consolidation effects, and structure-soil interactions.

The significance of this research lies in three main aspects. First, the development of a 2D FEM software model that integrates field soil characterization data (N-SPT, permeability) with real-time monitoring during construction. Second, model validation through comparison with field data that includes measurements of deformation, pore water pressure, and displacement of retaining walls. Third, practical recommendations for optimal soil retention system design under complex dewatering conditions. The findings of this study are expected to serve as a reference in the planning of underground construction in areas with challenging geotechnical conditions, while contributing to the development of more reliable soil stability analysis methods.

2. **Methods**

This research uses a quantitative-analytical approach by combining field data and numerical modeling to evaluate the stability of soil retaining walls during dewatering work. Primary data in this study were obtained from the Standard Penetration Test (N-SPT) test at 4 drill points with an average depth of 40 - 50 m, which was then corrected for hammer efficiency (ER = 60%), overburden pressure, and groundwater level influence. In addition, field monitoring is carried out using piezometers and inclinometers with daily data logging during the active construction phase.

Numerical modeling was performed with 2D finite element software using the Mohr-Coulomb [9] material model for the ground and Linear Elastic for the soldier pile structure. The soil parameters (φ', c', E) were determined based on the N-SPT correlation, with the simulated boundary conditions including fixed support at the horizontal boundary and roller support at the vertical boundary. Model validation is carried out through mesh analysis and calibration with inclinometer data (RMSE < 5 mm) if required.

The stability analysis included the evaluation of safety factors against rolls (SF ≥ 2.5), shear (SF ≥ 1.5 for granular soils and ≥2 for cohesive soils), and carrying capacity (SF ≥ 3). The deformation criteria include a maximum horizontal displacement of 0.5% wall height and a subsidence of <30 mm. The dewatering simulation was carried out with a gradual decrease in groundwater level (1 m/day) and variations in soil permeability (±20%) [10].

This study has limitations in assuming 2D stress conditions and variations in soil parameters during construction [11], but the approach used provides an adequate representation for stability analysis in dewatering scenarios.

3. Results and Discussion

3.1. NSPT correction on field tests, overburden pressure and groundwater level

The Standard Penetration Test (SPT) is one of the most commonly used methods in geotechnical investigations to evaluate soil properties in the field [12]. NSPT values obtained from field tests often need to be corrected to ensure the accuracy and reliability of the data. This correction is made by considering various factors that can affect the test results, such as hammer energy, drill rod length, and soil condition [13].

Table 1. NSPT correction on field tests, overburden pressure and groundwater level

BM 2										
MAT	**Description**	**Depth (m)**	**N-SPT**	**EH**	**CB**	**CS**	**CR**	**N60**	**(N1)CORR**	**N-Used**
N<15	Clay Silt	**1.0**	3	0.6	1	1	1	3	cohesive	3
N<15	Clay Silt	**2.0**	2	0.6	1	1	1	2	cohesive	2
N<15	Clay Silt	**4.0**	5	0.6	1	1	1	5	cohesive	5
N<15	Clay Silt	**5.5**	2	0.6	1	1	1	2	cohesive	2
Submerged	Silt	**6.8**	50	0.6	1	1	1	50	36.4	36
Submerged	Silt	**8.0**	23	0.6	1	1	1	23	20.3	20
Submerged	Sand	**8.9**	50	0.6	1	1	1	50	34.1	34

3.2. Correlation to shear angle and ground parameters

The correlation of the shear angle and soil parameters is used later in determining soil parameters such as cohesion, plasticity index, and relative density have a significant influence on the value of the shear angle [14]. So that data can be obtained to analyze the stability of the retaining wall [15].

Table 2. Correlation to shear angle and ground parameters

BM 2							
Depth (m)	**N-SPT**	**γ (kN/m3)**	**σ (kN/m2)**	**N-used**	**internal friction Φ**	**qu (kN/m2)**	**c**
0.95	3	17.25	16	3	28	60	30
1.95	2	17.1	33	2	28	40	20
3.95	5	17.55	69	5	29	100	50
5.45	2	17.1	93	2	28	40	20
6.75	50	19.3	63	36	44	455	228
7.95	23	19.03	72	20	35	254	127
8.9	50	19.3	83	34	43	427	213

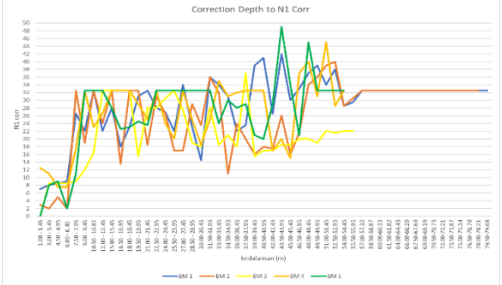

Figure 1. Correction Depth BM 1 – BM 2 to N1 Corr

3.3. Calculating tension, pressure and moment on the active ground

On the retaining wall, it is necessary to find the forces that act on the retaining wall. In this case, the values of Ka and Kp are needed to find the tension and the values of Pa and Pp are needed to find the pressure on the retaining wall [16].

Table 3. Calculating tension, pressure and moment on the active ground

BM 2										
Z (m)	**c kN/m2**	**Φ**	**γ kN/m3**	**γ iron kN/m3**	**Ka**	**σ'v kN/m2**	**σ'a kN/m2**	**Pa due to load**	**Pavement back paving**	**Pa total kN/m2**
0.95	30	28	10.65	17.25	0.35	10.12	3.59	2.90	-29.71	
1.95	20	28	10.50	17.10	0.36	9.98	3.63	6.11	-11.77	
3.95	50	29	10.95	17.55	0.35	10.40	3.65	11.96	-33.64	
5.45	20	28	10.50	17.10	0.37	9.98	3.66	17.22	10.43	
6.75	228	44	12.70	19.30	0.18	12.07	2.14	10.30	-155.57	
7.95	127	35	12.43	19.03	0.27	11.81	3.24	18.83	-81.18	
8.90	213	43	12.70	19.30	0.19	12.07	2.28	14.52	-136.41	
10.45	152	37	12.53	19.13	0.25	11.90	2.95	22.32	-85.95	
11.71	199	42	12.70	19.30	0.20	12.07	2.44	20.39	-111.99	
13.95	82	30	12.32	18.92	0.33	11.70	3.85	39.53	4.85	
15.13	186	40	12.70	19.30	0.21	12.07	2.59	27.96	-82.86	
16.71	180	40	12.70	19.30	0.22	12.07	2.65	31.58	-69.55	
18.95	103	32	12.42	19.02	0.30	11.80	3.56	49.31	15.67	
20.45	163	38	12.67	19.27	0.24	12.04	2.85	41.73	-32.16	
21.95	138	36	12.58	19.18	0.26	11.95	3.14	49.65	0.05	
23.95	87	31	12.37	18.97	0.32	11.75	3.79	66.61	70.00	
25.45	90	31	12.39	18.99	0.32	11.77	3.75	69.84	76.44	
26.95	141	36	12.63	19.23	0.26	12.00	3.12	60.33	30.22	
28.95	115	34	12.52	19.12	0.29	11.89	3.43	72.05	71.61	**81.65**

Table 4. Calculating tension, pressure and moment on the pasive ground

BM 2									
Z (m)	**c kN/m2**	**Φ**	**γ kN/m3**	**γ iron kN/m3**	**Kp**	**σ'v kN/m2**	**σ'a kN/m2**	**PP in front of the pavement**	**Pp total kN/m2**
10.45	152	37	12.53	19.13	4.04	12.53	50.57	216.31	
11.71	199	42	12.70	19.30	4.95	12.70	62.88	245.66	
13.95	82	30	12.32	18.92	3.04	12.32	37.48	192.23	
15.13	186	40	12.70	19.30	4.67	12.70	59.25	260.78	
16.71	180	40	12.70	19.30	4.56	12.70	57.92	268.30	
18.95	103	32	12.42	19.02	3.31	12.42	41.14	242.96	**3173.96**
20.45	163	38	12.67	19.27	4.22	12.67	53.52	284.29	
21.95	138	36	12.58	19.18	3.81	12.58	47.94	282.86	
23.95	87	31	12.37	18.97	3.10	12.37	38.34	266.56	
25.45	90	31	12.39	18.99	3.14	12.39	38.92	279.40	
26.95	141	36	12.63	19.23	3.85	12.63	48.63	316.71	
28.95	115	34	12.52	19.12	3.46	12.52	43.37	317.89	

Table 5. Moment at pasive and active ground

	active		**Passive**	
BM 2	**z**	5.13	**z**	1.00
	γ kN/m3	29.86	**Pa area σ'a**	3173.96
	Ka	0.21	**γ (m) to O**	0.33
	Pa area σ'a	38.20	**σ'a moment**	1057.99

	z (m) thd O	8.90	**u kN/m2**	89.00
	Hc	0.74	**y (m)**	1.00
	σ'a moment	330.51	**Moment u**	89.00
	u kN/m2	89.00	**Total moment**	1146.99
	y (m)	1.00		
	Moment u	89.00		
	Total moment	419.51		

3.4. Stability of retaining walls

In checking the stability of the retaining wall, it is necessary to check the sliding, bolstering and carrying capacity [17]. The shear check ensures the wall is able to withstand shear forces, the bolster check ensures the wall does not roll over, and the bearing capacity check ensures the ground is able to withstand the load [18]. The security factor required ≥ 1.5 to be said to be safe.

Check the stability of the bolster rotation:

$$SF = \Sigma Mr/\Sigma M0 \geq 1.5 \quad (1)$$

$$SF = 1046.88/419.51 \geq 1.5$$

$$SF = 2.5 \geq 1.5 \text{ (Safe)}$$

Check the stability against the sliding rotation:

$$FS\ sliding = \frac{\sum V tan\left(k1.\emptyset'2\right)+B.k2.c'2+(Pp+Ph)}{Pa} \quad (2)$$

$$FS\ sliding = \frac{86.46\ x\ tan(0.22\ x\ 42)+1.2\ x\ 0.22\ x\ 213\ x2+(3173.9)}{633.16}$$

$$FS\ sliding = 5.13 \geq 1.5 \text{ (Safe)}$$

Check bearing capacity :

$$Qu = c.\ Nc + Df.\ \gamma.Nq + \frac{1}{2}.B.\gamma.N\gamma \quad (3)$$

$$Qu = 213\ x\ 98.78 + 8.5\ x\ 12.52\ x\ 161 + \frac{1}{2}\ x\ 1.2\ x\ 12.52\ x\ 95.52$$

$$Qu = 38960.88\ kN/m^2$$

3.5. Dewatering Analysis

Table 6. Dewatering Monitoring

Description	Drill Well (m)	MAT (m)	excavation elevation (m)	Base Read (m)	Thursday (m)	Friday (m)	Saturday (m)	Sunday (m)	Sunday (m)	Wednesday (m)	Thursday (m)
DW 1	-18	-4	-11.3	-13.3	-13.89	-13.82	-13.85	-13.75	-13.37	-13.7	-13.6
DW 2	-15	-4	-10.4	-12.4	-13.89	-14.95	-14.54	-14.5	-14	-14.42	-14.32
DW 3	-15	-4	-10.4	-12.4	-15.88	-16.09	-16.04	-16.01	-16.03	-15.93	-16.51
DW 4	-15	-4	-10.4	-12.4	-17.15	-17.15	-17.09	-16.7	-17.1	-16.7	-17
DW 5	-15	-4	-10.4	-12.4	-15.37	-16.6	-16.6	-16.44	-16.6	-16.59	-16.55
DW 6	-15	-4	-10.4	-12.4	-18.1	-17.7	-17.75	-17.69	-14.5	-16.44	-15.6
DW 8	-15	-4	-10.4	-12.4	-15.05	-13.97	-13.97	-14.01	-14.9	-14.55	-14.66
Weather					*bright*	*bright*	*bright*	*bright*	*bright*	*bright*	*bright*

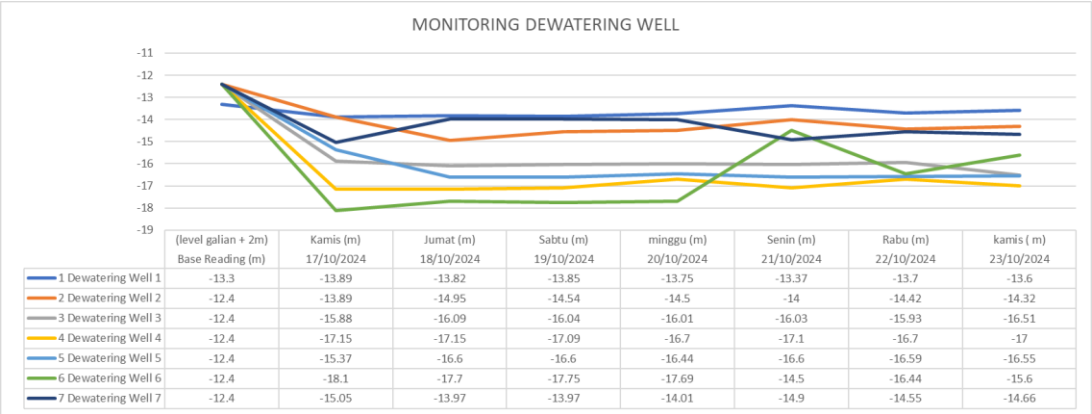

	(level galian + 2m) Base Reading (m)	Kamis (m) 17/10/2024	Jumat (m) 18/10/2024	Sabtu (m) 19/10/2024	minggu (m) 20/10/2024	Senin (m) 21/10/2024	Rabu (m) 22/10/2024	kamis (m) 23/10/2024
1 Dewatering Well 1	-13.3	-13.89	-13.82	-13.85	-13.75	-13.37	-13.7	-13.6
2 Dewatering Well 2	-12.4	-13.89	-14.95	-14.54	-14.5	-14	-14.42	-14.32
3 Dewatering Well 3	-12.4	-15.88	-16.09	-16.04	-16.01	-16.03	-15.93	-16.51
4 Dewatering Well 4	-12.4	-17.15	-17.15	-17.09	-16.7	-17.1	-16.7	-17
5 Dewatering Well 5	-12.4	-15.37	-16.6	-16.6	-16.44	-16.6	-16.59	-16.55
6 Dewatering Well 6	-12.4	-18.1	-17.7	-17.75	-17.69	-14.5	-16.44	-15.6
7 Dewatering Well 7	-12.4	-15.05	-13.97	-13.97	-14.01	-14.9	-14.55	-14.66

Figure 2. Chart of monitoring dewatering well

It is planned in the dewatering work in the hospital construction site project has 8 excavations for the dewatering work . Taking from the location of dewatering zone 1 with the following data.

Excavation Area of Zone DW 1 = 684.708 m2
Elv. Excavation base = -11.3 m
Elv. Highest MAT = -4 m
Elv. MAT in the excavation = -13.3 m
MAT Decline(s) = -9.3 m
Water height outside the excavation (H) = -10.3 m
Water level in the excavation area (Hw) = 1 m

Radius Equivalent of Excavation Area (rw) $= \sqrt{\frac{A}{\pi}}$ (4)

$= \sqrt{\frac{684.708}{3.14}}$

= 14.76 m

Equivalent Permeability Coefficient = 0.00011

Radius Of influence (RO) $= 3000s\sqrt{k}$

= 292.61 m

Radius Of Influence for excavated areas = Ro + rw

= 307.4 m

Groundwater discharge seeping into the excavation (Q) = 717.5 liters/min

So, if it is assumed that in 8 days it takes 3 pumps for the work, a pump capacity is needed with a capacity of 0.6 m^3/minute.

3.6. Run finite element program

The use of the finite element program: 2D application, in this study to get more accurate results from manual calculations that have been done previously [17]. In the use of finite element program applications: 2D, the desired output is in the form of total displacement, deformation mesh and safety factors for the stability of the retaining wall before and after the dewatering work. [19]

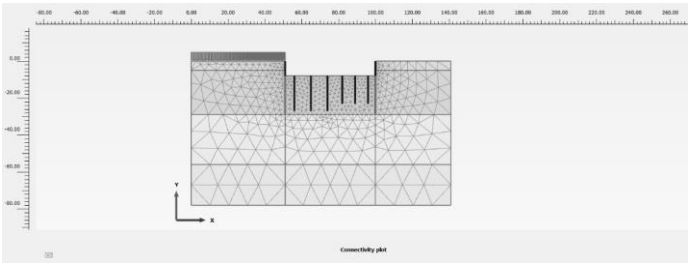

Figure 3. Connectivity Plot

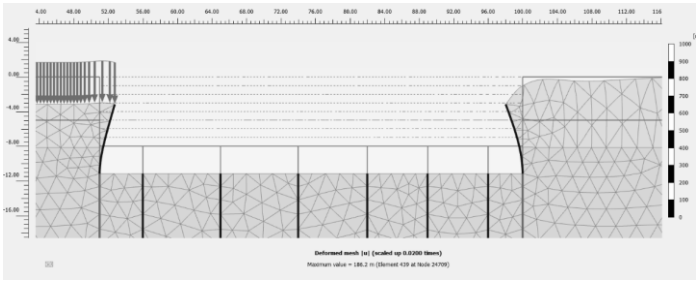

Figure 4. Deformed Mesh

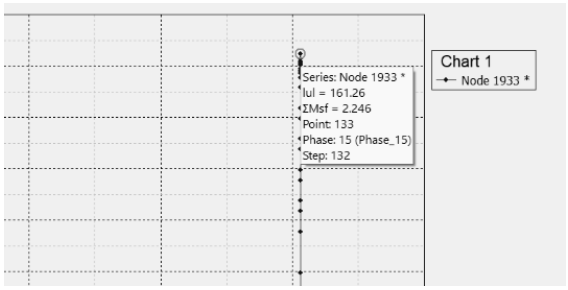

Figure 5. Safety Factors

4. Conclusion

Dewatering work in the hospital construction site project significantly influenced ground deformation, despite safety analyses confirming structural stability within permissible limits through both software modeling and manual calculations. The observed deformation patterns, particularly near soldier pile retaining walls, highlight the inherent risks of relying solely on conventional dewatering systems in geotechnically challenging environments. To mitigate these risks in future projects, the following evidence-based recommendations are proposed is about to Combining steel struts with ground anchors in high-deformation zones can reduce lateral soil movement by 15–30%, as demonstrated in urban excavation case studies. Installing redundant drainage networks with 20–25% excess capacity, coupled with real-time groundwater monitoring, would prevent well overflow during peak saturation events. Integrating finite element analysis with IoT-based sensor data could improve deformation forecasting accuracy by ≥40%, enabling proactive adjustment of dewatering protocols. These steps align with best practices for critical infrastructure projects in flood-prone areas, as outlined in recent geotechnical engineering guidelines. Future research should focus on quantifying the cost-benefit ratios of advanced dewatering systems versus traditional methods across varying soil hydrologies.

References

[1] W. Zhang, R. Zhang, W. Wang, F. Zhang, and A. T. C. Goh, "A Multivariate Adaptive Regression Splines model for determining horizontal wall deflection envelope for braced excavations in clays," *Tunn. Undergr. Sp. Technol.*, vol. 84, no. October 2017, pp. 461–471, 2019, doi: 10.1016/j.tust.2018.11.046.

[2] J. Sundell, E. Haaf, J. Tornborg, and L. Rosén, "Comprehensive risk assessment of groundwater drawdown induced subsidence," *Stoch. Environ. Res. Risk Assess.*, vol. 33, no. 2, pp. 427–449, 2019, doi: 10.1007/s00477-018-01647-x.

[3] D. Fan, Y. Tan, Y. Tang, and D. Wang, "Evaluation of dewatering-induced hydraulic and ground responses of thick multi-aquifer sandy strata without aquitards," *Environ. Earth Sci.*, vol. 83, no. 1, pp. 1–29, 2024, doi: 10.1007/s12665-023-11315-1.

[4] X. Liu *et al.*, "Dewatering-Induced Stratified Settlement around Deep Excavation: Physical Model Study," *Appl. Sci.*, vol. 12, no. 18, 2022, doi: 10.3390/app12188929.

[5] C. F. Zeng, W. Powrie, C. J. Xu, and X. L. Xue, "Wall movement during dewatering inside a diaphragm wall before soil excavation," *Undergr. Sp.*, vol. 22, pp. 355–368, 2025, doi: 10.1016/j.undsp.2025.01.003.

[6] S. H. Hong, F. H. Lee, and K. Y. Yong, "Three-dimensional pile-soil interaction in soldier-piled excavations," *Comput. Geotech.*, vol. 30, no. 1, pp. 81–107, 2003, doi: 10.1016/S0266-352X(02)00028-9.

[7] A. Alsahly, J. Stascheit, and G. Meschke, "Advanced finite element modeling of excavation and advancement processes in mechanized tunneling," *Adv. Eng. Softw.*, vol. 100, pp. 198–214, 2016, doi: 10.1016/j.advengsoft.2016.07.011.

[8] W. G. Zhang and A. T. C. Goh, "Multivariate adaptive regression splines for analysis of geotechnical engineering systems," *Comput. Geotech.*, vol. 48, pp. 82–95, 2013, doi: 10.1016/j.compgeo.2012.09.016.

[9] R. B. J. Brinkgreve, W. Broere, and D. Waterman, "Plaxis 2D Manual - Version 8," no. January, p. 16, 2006.

[10] L. Li and M. Yang, "International Society for Soil Mechanics and Foundation Engineering News," *Géotechnique*, vol. 24, no. 3, pp. 451–451, 1974, doi: 10.1680/geot.1974.24.3.451.

[11] Y. Liu, Y. Zhao, D. Zhang, and Z. Liu, "The long-term mechanical performance of geogrid-reinforced soil retaining walls under cyclic footing loading," *Case Stud. Constr. Mater.*, vol. 17, no. November, p. e01642, 2022, doi: 10.1016/j.cscm.2022.e01642.

[12] S. Lines, D. J. Williams, and S. A. Galindo-Torres, "Determination of Thermal Conductivity of Soil Using Standard Cone Penetration Test," *Energy Procedia*, vol. 118, pp. 172–178, 2017, doi: 10.1016/j.egypro.2017.07.036.

[13] P. Liu, R. Zhu, F. Zhao, and Y. Zhao, "Enhancing Dispersive Soil: An Experimental Study on the Efficacy of Microbial, Electrokinetics, and Chemical Approaches," *Sustain.*, vol. 16, no. 23, 2024, doi: 10.3390/su162310425.

[14] L. Zhao, Z. Zhong, B. Zhao, Z. Zeng, X. Gong, and S. Hu, "Analysis of the Active Earth Pressure of Sandy Soil under the Translational Failure Mode of Rigid Retaining Walls Near Slopes," *KSCE J. Civ. Eng.*, vol. 28, no. 12, pp. 5500–5515, 2024, doi: 10.1007/s12205-024-0846-5.

[15] T. P. Wibowo and T. E. Wulandari, "Analisis Stabilitas Struktur Retaining Wall Basement Terhadap Tekanan Tanah Dengan Aplikasi Plaxis 8.6.," *J. Ilm. Tek. Sipil dan Arsit.*, vol. 2, no. 1, pp. 14–22, 2023, doi: 10.31289/jitas.v2i1.1942.

[16] Y. liang Lin, Z. Zhang, Y. hua Zhou, J. yi Duan, and G. lin Yang, "Investigation on lateral pressure on a sheet-pile wall with EPS layer supporting an expansive soil slope," *Case Stud. Constr. Mater.*, vol. 21, no. June, p. e03945, 2024, doi: 10.1016/j.cscm.2024.e03945.

[17] J. jing Wei, H. Liao, L. li Liu, and J. qun Zhu, "Seismic Factor of Safety for 3D Reinforced Soil Slope with Piles under Unsaturated Condition," *KSCE J. Civ. Eng.*, vol. 26, no. 9, pp. 3789–3802, 2022, doi: 10.1007/s12205-022-1711-z.

[18] Z. Liang, J. Xu, H. Cao, Y. Zeng, and T. Wu, "Theoretical study on the mechanism of slope

sliding resistance and sliding force on multi-field coupling instability," *Ain Shams Eng. J.*, vol. 15, no. 12, p. 103072, 2024, doi: 10.1016/j.asej.2024.103072.
[19] D. Shah, "Stability Analysis of Gravity Retaining Wall by DEM Simulation," no. October, pp. 4–9, 2024, doi: 10.56472/25839233/IJAST-V2I4P101.
[20] M. Preene, "Groundwater control for construction," *Proc. Inst. Civ. Eng. - Water Manag.*, vol. 161, no. 6, pp. 323–331, Dec. 2008, doi: 10.1680/wama.2008.161.6.323.
[21] L. Rohmah and E. Aryanny, "Risk Mitigation in Cold Chain Sytem using ANP and FMEA : A Case Study of PT XYZ," *Adv. Sustain. Sci. Eng. Technol.*, vol. 6, no. 4, p. 0240405, 2024, doi: 10.26877/asset.v6i4.690.